The Penguin Feather as Inspiration for Anti-Icing Surfaces

Michael J. Wood[1], Gregory Brock[1], Anne-Marie Kietzig[1*]

[1] *McGill University Department of Chemical Engineering, Montréal Canada*

*Corresponding author: anne.kietzig@mcgill.ca

Abstract—**There has been much effort in the past few decades towards engineering surfaces which passively shed ice. Strategies toward this goal have included low surface energy chemical coatings and air-trapping superhydrophobic texturing. These strategies have proven to lack efficacy and/or robustness against repeated cycles of icing/de-icing. There is growing consensus that the two aspects of anti-icing surfaces (water-shedding and ice-shedding) require two distinct design strategies. Nature contrarily does not rely on low energy coatings to achieve water-shedding or ice-shedding characteristics. An excellent example of a natural anti-icing surface is the body feather of the sub-Antarctic penguin, which ornithologists have noted is perpetually free of ice despite these birds hunting in frigid waters and the temperature of their outer plumage being below the freezing point. Recent research has indicated that some of this anti-icing effect is due to the hierarchical structure of the body feather imparting a water droplet-shedding effect.**

In this work, we explore the ice-shedding characteristics of the penguin body feather structure. We show that the ice adhesion properties of this natural example are distinct from its water adhesion properties. Millennia of trial-and-error evolutionary experiments have devised a structure which induces facile cracking at the ice-feather interface. The branching wire-like morphology of the penguin body feather barbs allow for movement at the surface's microstructural level which we conjecture results in facile opening of these beneficial interfacial cracks. Such a mechanism which does not rely on surface chemistry or maintaining a trapped air cushion is inherently robust and efficient.

The ice-shedding design strategies we have uncovered in this natural example are then tested on metallic biomimetic substrates. The curved barb structure which makes up the penguin body feather is mimicked using ultra-fine woven stainless-steel wire cloths. We show that such a 3-dimensional microstructural network imparts remarkable ice-shedding performance in the synthetic surface compared to flat, polished, monolithic surfaces of the same stainless-steel. In carrying out this work, we show that robust ice-shedding surfaces can be fabricated out of bare metal if one considers the actual mode of ice-substrate failure – much like nature's solutions do.

Keywords— ***Ice-Shedding, Biomimetic, Anti-Icing, Ice Adhesion, Fracturing***

I. Introduction

The accumulation of ice on the surface of external structures has been a persistent engineering challenge. For example, ice accretion can cause power transmission lines to fail under excess weight [1], solar panels to lose their transmissivity [2], asphalt roads and pavements to lose their traction [3], and airfoils to lose their capacity to lift [4]-[7]. Such a widespread and consequential problem has spawned much research in recent decades towards the development of surfaces which passively inhibit the accretion of surface ice. The "anti-icing" strategies employed in the literature can be broadly categorized into: (i) prevention of the formation of ice altogether (i.e. water-shedding); or (ii) the lowering of ice adhesion strength (i.e. ice-shedding).

There is growing consensus that the two anti-icing surface design strategies are distinct, where the adhesion of liquids is decidedly different than the adhesion of solids. On the one hand, water-shedding functionality requires hierarchical roughness and favourable surface chemistry [8]. The water-solid contact time and contact area of droplets impinging on such a surface is limited, preventing the formation of ice [9]. On the other hand, a wetting transition can occur under cold, humid conditions where water penetrates the surface roughness which had once trapped air. Often superhydrophobic surfaces present with increased ice adhesion strengths due to the interlocking effect that the ice has with the hierarchical roughness [10]. To overcome these limitations, some have researched the infusion of non-miscible lubricants into roughened surfaces to facilitate the shedding of both water and ice [11]-[14]. However, these surfaces have been shown to lack robustness even in laboratory testing [6], [15].

Recent progress has shown that the induction of interfacial cracks is key to the engineering of passive ice-shedding surfaces [16]-[20]. In fact, fracture mechanics principles have allowed for the design of ice-shedding surfaces out of metals without any additional chemical coatings [21], [22]. Specifically, woven wire cloths have been reported to have exceptionally low ice adhesion strengths due to the initiation of microcracks at each weave and facile opening of these cracks along the path of the wires [21].

It is evidently difficult to combine the disparate functionalities of water-shedding and ice-shedding into a single, robust, synthetic surface. However, nature may offer us an excellent design strategy through the body feather of sub-Antarctic penguins. These birds are seldom seen to carry macroscopic ice on their outer plumage despite them hunting in frigid waters, and their feathers offering such insulation that their outer surface temperatures match the freezing environmental conditions in which they live [23]-[26]. The anti-icing functionality of the circumpolar penguin feather has been at least partially attributed to the robust water-shedding characteristics of their hierarchically rough three-dimensional wire-like structure. While keratin – the structural protein of the feathers – is hydrophilic, water

droplets on the surface of the plumage assume a Cassie-Baxter wetting state because of air entrapment in the voids of the micro- and nano-texturing of the feather [23], [26]. Furthermore, it is known that the hydrophobicity of seabird feathers is improved through the application of preen oil by combing with their beaks. However, it is still unclear if preen oil improves hydrophobicity directly by providing the feathers a lipid layer, or functions simply by maintaining feather structure [27]. For example, Bormashenko et al. have shown that water droplets placed on pigeon feathers assume a Cassie-Baxter wetting state even after removing any oils with ethanol [28].

In this work, we investigate the ice-shedding performance of sub-Antarctic penguin feathers, which to the authors' knowledge has not been previously reported. The lessons learned by experimenting with the natural example of the penguin feather are then used to develop a robust biomimetic anti-icing surface which combines water-shedding and ice-shedding functionality.

II. Experimental

A. Penguin Feather Preparation

Freshly moulted body feathers of the sub-Antarctic Gentoo penguin *Pygoscelis papua* were collected and supplied by the Montréal Biodôme. These specimens were first used as-received without any cleaning to test the effect of any preening oil which might remain on their surface. As shown in Fig. 1 (a), the body feathers of the *Pygoscelis papua* are arranged in an overlapping pattern, creating a plumage mat. We replicated this natural surface by arranging individual moulted feathers in overlapping rows on a roughened stainless-steel plate using small dabs of epoxy, as shown in Fig. 1 (b).

Fig. 1 (a) Photograph of a specimen, showing the overlapping layered structure of its body feathers. (b) Reconstruction of moulted body feathers into a layered structure resembling that of a sub-Antarctic penguin.

B. Biomimetic Surface Preparation

Ultra-fine 316 stainless-steel Dutch weave filter cloths (Dorstener Wire Tech., Inc.) of mesh number 200x1400 were used as the synthetic substrate in this work. A control surface of 0.036"-thick 316 stainless-steel with an ASTM #8 finish (McMaster-Carr Supply Co.) was also tested. All metallic substrates were ultrasonically cleaned first in a lactic acid-based detergent, *CLR* (Jelmar, LLC.), then in acetone before any further manipulation.

The cleaned stainless-steel filter cloths were decorated with laser-induced periodic surface structures (LIPSS) by irradiation with ultrashort laser pulses. A peak intensity of 696 $W \cdot cm^{-2}$, pulse fluence of 0.70 $J \cdot cm^{-2}$, and effective number of pulses-per-spot of 200 were used. The specifics of this laser micromachining routine have been reported in our previous work [29].

The LIPSS-decorated surface destined to become water-wicking were placed in a bath of boiling deionized water for 48 hours after micromachining. The LIPSS-decorated surface destined to become water-shedding were first ultrasonically cleaned in ethanol for 5 minutes to remove nanoparticles, then exposed to CO_2 in a heated reactor at 25 PSI and 60 °C for 48 hours. The resulting surface, as discussed in our previous work, presents as water-shedding after subsequent exposure to lab air for 30 days [29].

C. Sample Characterization

All the natural and biomimetic substrates described in the previous sub-sections were imaged using a *Quanta 450* scanning electron microscope (ThermoFisher, Inc.). The natural penguin feathers were first sputter-coated with 5-10 nm of gold to render them conductive before SEM imaging.

Water contact angle measurements were performed using a lab-built goniometer. The advancing and receding contact angles were measured by first gently placing a 2 µl water droplet onto the studied surface, then pumping and withdrawing, respectively, 5 µl from said droplet at a rate of 0.25 µl/s. All goniometric measurements were repeated at five different locations on the surfaces.

The procedure for the ice adhesion measurements has been extensively described in a previous publication [21]. In brief, the studied surface is clamped into a thermoelectric cooling plate set at -15 °C. After letting the system reach the set temperature, 2500 µl of chilled reverse osmosis water (-5 – 0 °C) is added dropwise to a borosilicate glass mould and allowed to freeze. Then a *ZPS-DPU-22* digital force probe (Imada, Inc.) is driven into the ice column at a rate of 0.5 mm/s. The ice adhesion strength is obtained by dividing the peak force measured by the cross-sectional area of the glass mould. Ice adhesion tests were repeated 5 times per substrate in the exact same location on their surface.

III. Results and Discussion

A. Morphology of Natural and Biomimetic Surfaces

A photograph and scanning electron micrographs of *Pygoscelis papua* sub-Antarctic penguin body feathers are presented in Fig. 2 (a) and (b). The structure of the feather is a smooth central rachis which divides two mirrored pinnae, as shown in Fig. 2 (a). The pinnae are composed of hierarchical wire-like structures, the largest of which are the parallel barbs, as shown in Fig. 2 (b_1). The barbs meet the

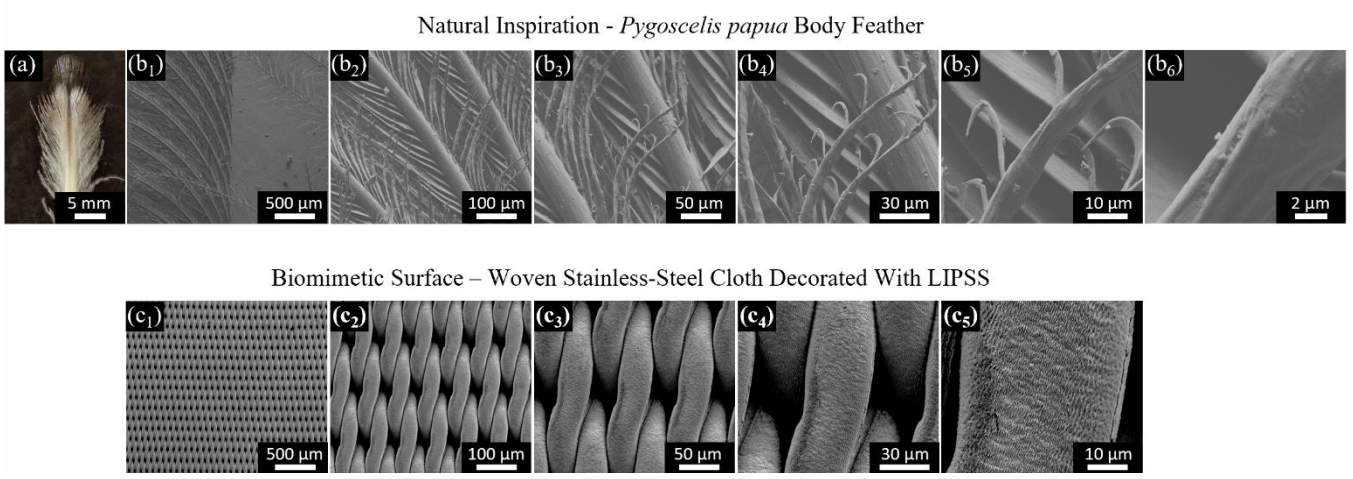

Fig. 2 (a) Photograph of the *Pygoscelis papua* body feather. Scanning electron micrographs of body feather (b_1) the rachis and barbs; (b_2) barbs and barbules; (b_3-b_5) barbules and hamuli; (b_6) oriented wrinkles on the barbules and hamuli. Scanning electron micrographs of stainless-steel wire cloth (c_1-c_3) overall woven structure; (c_4-c_5) single weft wire decorated with oriented laser-induced periodic surface structures.

central rachis at an angle of 15 – 20° and have a diameter of 30 – 35 µm. As shown in Fig. 2 (b_2), the barbs themselves divide mirrored sets of branching barbules. These barbules have a diameter of 10 – 15 µm and meet the barbs at an angle of 20 – 25°. Zooming further in Fig. 2 (b_3-b_5) reveals that some of the barbules have hooked hamuli arranged along them with diameters of 2 – 5 µm. These hamuli help to create an interlocked rigorous three-dimensional microstructural network when the bird preens itself [23]. Furthermore, the high magnification scanning electron micrograph of Fig. 2 (b_6) reveals that the hamuli and barbules are decorated with nanoscale wrinkles, oriented along their central axes.

Fig. 2 (c) next presents the morphology of the stainless-steel biomimetic surface. Fig. 2 (c_1) shows a high-level scanning electron micrograph of the woven wire cloth material, demonstrating the regular, repeating three-dimensional microstructural network of the Dutch weave. This material is composed of warp wires running the width of the cloth, and perpendicular weft wires (visible in the SEM) woven above and below two adjacent warp wires. Fig. 2 (c_2-c_3) present higher magnifications of the woven wires. The weft wires of this material have a diameter of 40 µm, matching well the diameter of the barbs of the penguin body feather. Finally, Fig. 2 (c_4-c_5) clearly show the results of the laser micromachining routine. The weft wires are decorated with highly ordered nanogratings (i.e. LIPSS) oriented along their central axes, much like the nanoscale wrinkles which cover the hamuli and barbules of the sub-Antarctic penguin body feather.

The comparison of Fig. 2 (b) and Fig. 2 (c) already shows the potential of a woven wire cloth to biomimic the form of the penguin body feather in shape and dimension. The basic three-dimensional network of wire-like structures is well copied from the natural example and the hierarchical texturing is included through the laser processing steps. The remainder of this work will explore if the anti-icing functions of the penguin body feather follow with this mimicked form in our synthetic surface.

B. Wettability of Natural and Biomimetic Surfaces

The first anti-icing surface functionality tested was water-shedding. These results are presented in Fig. 3. We first tested the wettability of stainless-steel and keratin as smooth surfaces. For stainless-steel, these were dynamic contact angle measurements taken on mirror-polished monolithic coupons; for keratin, these were dynamic contact angle measurements taken on the feather's rachis. As summarized in Fig. 3, the smooth stainless-steel presents with hydrophilic contact angles, and has a rather large contact angle hysteresis (33 ± 4°). While the smooth keratin presents with a higher advancing contact angle, it also has a large measured contact angle hysteresis (33 ± 6°).

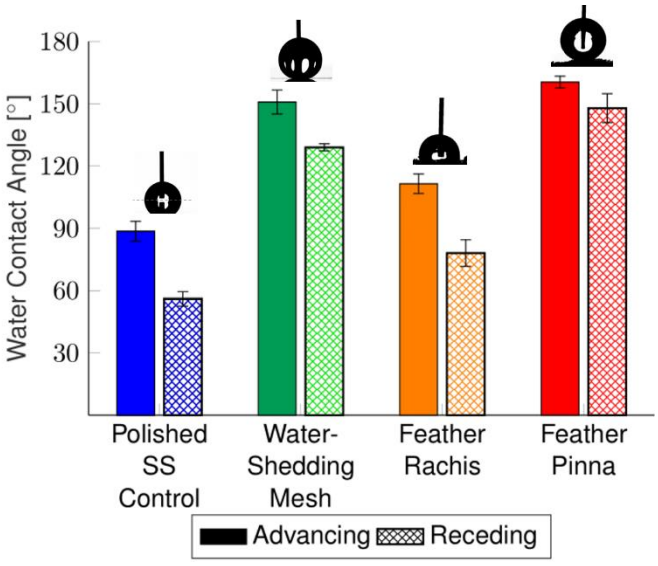

Fig. 3 Advancing and receding contact angles measured on the: polished stainless-steel control, smooth feather rachis, hierarchically textured feather pinna, and water-shedding biomimetic mesh surfaces. No wettability data are presented here for the water-wicking mesh surface as water droplets present with contact angles of 0°, completely wetting the surface. Error bars show 95% confidence intervals on the mean.

The water-shedding phenomenon observed on the sub-Antarctic penguin body is therefore not a result of feather material of construction. Rather, as demonstrated in Fig. 3, the hierarchical roughness found in the feather pinnae introduces air-trapping effects, leading to a Cassie-Baxter wetting state. The wire-like morphology of the feather pinnae barbs and barbules which are covered in nanoscale wrinkles has resulted in a measured advancing contact angle of 160 ± 3° and a measured receding contact angle of 148 ± 7°. Referring to Fig. 1 (a), one can see that the feathers are arranged on the penguin body such that smooth rachi are completely covered by overlapping pinnae. Moreover, the effect of the hierarchical roughness of keratin on surface wettability matches well what has been reported for pigeon feathers [28]. The dynamic contact angle results for the feather's pinnae also matches well what has been reported for other species of penguin feathers [23], [26].

The combination of hierarchical roughness and favourable surface chemistry found on the sub-Antarctic penguin feather is well mimicked by the laser-irradiated stainless-steel mesh. As presented in Fig. 3, the LIPSS-decorated mesh which was exposed to CO_2 in a heated reactor has been rendered water-shedding. This surface presents with an advancing contact angle of 151 ± 6° and a receding contact angle of 129 ± 2°. The woven wire-like structure with highly oriented nanoripples and low-energy carbonaceous surface chemistry indeed introduces air-trapping effects like the penguin feather.

Not shown in Fig. 3 are the water contact angle measurements taken on the LIPSS-decorated mesh which was exposed to boiling water. This hierarchically-rough surface with a high surface energy hydrophilic layer has been rendered completely water-wicking with no sessile, advancing, nor receding contact angle measurable. Contacting water completely penetrates the three-dimensional microstructural network

C. Ice-Shedding Performance of Natural and Biomimetic Surfaces

We next moved on to testing the ice adhesion performance of our reconstructed *Pygoscelis papua* plumage mat. The first set of measurements were done with the as-received body feathers, those which would have some preen oil still on them from the last time the bird had combed itself. As shown in Fig. 4, the feathers with preen oil very easily shed adhered ice, with an average measured ice adhesion strength of 20 ± 16 kPa.

We noted that for the vast majority of our experiments with the penguin body feathers, the dislodged ice column was free of any feather debris, as in Fig. 5 (a). Here the dislodged ice has a very distinct imprint of the feather mat left in it. That is to say that the low ice adhesion strengths measured are not the result of the feathers being ripped apart upon the application of the ice dislodging force. Rather, such a low adhesion strength stems from facile failure at the feather-ice interface.

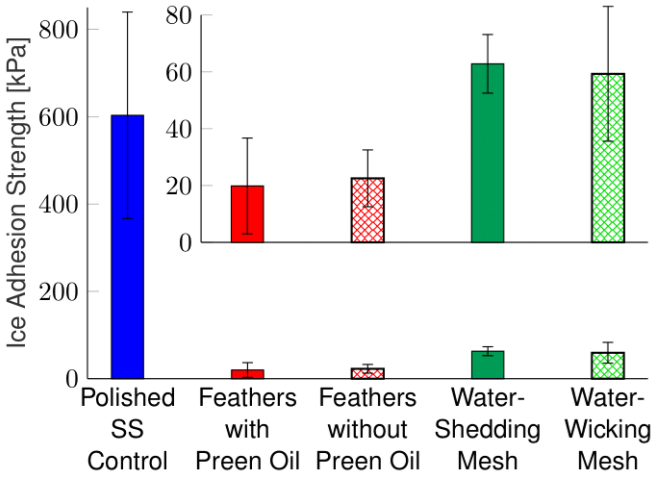

Fig. 4 Ice adhesion strength measured on the: reconstructed plumage mat with preen oil, reconstructed plumage mat with preen oil removed, water-shedding biomimetic stainless-steel mesh, and water-wicking stainless-steel mesh in comparison with a flat polished stainless-steel control sample. Error bars shown 95% confidence intervals on the mean.

There were, however, some instances where wisps of feather were seen attached to the dislodged ice column. An example of such a surface is given in Fig. 5 (b). In none of these cases were the measured ice adhesion strengths exceptionally low. Furthermore, the ice adhesion strength showed no increasing nor decreasing trend with number of de-icing cycles. We conjecture that rather than the forces of ice dislodging being the direct cause of feather degradation, it is simply coincidental aging of the feathers which caused them to fall apart. As discussed by Moreno-Rueda, the role of the ritual of preening is theorized to help maintain the feather structure [27].

We explored the role of preen oil beyond feather maintenance by measuring the ice adhesion strength of our reconstructed plumage mat with preen oil removed. The oil was removed by ultrasonically cleaning the reconstructed plumage mat in ethyl alcohol, as per the methods of Bormashenko et al. [28]. As shown in Fig. 4, the feather surface shows no statistically-significant change in ice adhesion strength with or without preen oil. The ice-shedding characteristics of the penguin body feather are the result of surface morphology, not lubrication at the interface.

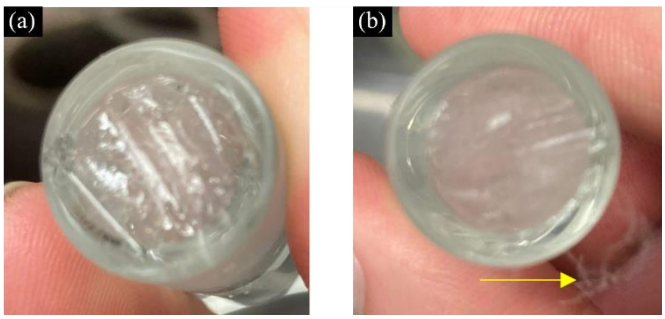

Fig. 5 (a) Underside of an ice column dislodged from the reconstructed plumage mat showing the imprint of the once adhered penguin feathers. (b) A dislodged ice column with a small feather piece attached to it.

Next, we tested the ice-shedding performance of our biomimetic surface. As shown in Fig. 4, the biomimetic water-shedding mesh presents with an average ice adhesion strength of 63 ± 10 kPa. This is an exceptional decrease compared to the polished stainless-steel control sample, which has an average ice adhesion strength of 603 ± 236 kPa. These results are especially interesting considering that this surface does not rely on low energy polymeric coatings, nor sacrificial lubricants which would need to be reapplied for continued efficacy.

We then explored the role of surface wettability on ice adhesion strength manifested by the hierarchically-textured stainless-steel wire cloths. Fig. 4 shows that there is no statistically-significant difference between the ice adhesion strengths measured on the water-wicking mesh and on the water-shedding mesh. The ice-shedding character of the biomimetic surface is not the result of air trapping in the three-dimensional microstructural network; the ice is cleanly shed even though it infiltrates the wire network. This behaviour matches very well that of the penguin feather where ice is shed with or without preen oil. The water-shedding and ice-shedding phenomena of the penguin body feather, and indeed our biomimetic surface, are derived from distinct functions of the hierarchical surface structure.

We hypothesize that in the case of both the sub-Antarctic penguin body feather and the biomimetic woven wire cloth, the facile ice shedding character is derived from the induction of microstructural movement upon application of the dislodging force. Such movement of the barbs/barbules (in the case of the natural surface) or weft wires (in the case of the synthetic surface) will lead to facile opening of interfacial cracks.

The results of this work show that the penguin body feather is in fact anti-icing due to two distinct functionalities: water-shedding and ice-shedding. Furthermore, these functionalities are not derived from ultra-low energy surface chemistries, but rather a clever three-dimensional wire-like network and hierarchical texturing.

IV. Conclusions

In this work, we investigated the anti-icing performance of body feathers of the sub-Antarctic Gentoo penguin *Pygoscelis papua*. We note that the anti-icing nature of the penguin is derived from two distinct functions of its body feathers. The first anti-icing function is water-shedding which is induced through air trapping in a three-dimensional wire-like structure that is in turn decorated with nanoscale wrinkles. The second anti-icing function is ice-shedding which is not the result of anti-wetting. We rather hypothesize that facile ice shedding is derived from microstructural movement of the wire-like network which induces cracks at the ice-feather interface.

We then mimicked the form and two distinct functions of the sub-Antarctic penguin body feather by decorating an ultra-fine stainless-steel Dutch weave filter cloth with laser-induced periodic surface structures (LIPSS). A water-shedding functionality is induced by the hierarchical texturing and low energy carbonaceous surface chemistry of the laser-irradiated mesh. An ice-shedding functionality is imparted by the wire network which induces interfacial cracks, but not by the surface chemistry. Our robust metallic biomimetic surface has an ice adhesion strength which is 90% lower than a flat monolithic sample of the same stainless-steel material.

Nature shows us that we must design for the two distinct problems of icing: water adhesion and ice adhesion. Millenia of evolutionary experiments have given us the example of the sub-Antarctic penguin body feather, which demonstrates that these two design strategies can be efficiently combined to engineer robust anti-icing surfaces.

Acknowledgment

The authors thank Dr. Emiko Wong of the Biodôme de Montréal for collecting and supplying the moulted penguin feather specimens.

References

[1] M. Farzaneh, C. Volat, and A. Leblond, "Anti-icing and De-icing Techniques for Overhead Lines," in *Atmospheric Icing of Power Networks*, M. Farzaneh Ed. Dordrecht: Springer Netherlands, 2008, pp. 229-268.

[2] R. Carriveau, R. Mailloux, A. Edrisy, and P. Cadieux, "Ice adhesion issues in renewable energy infrastructure," *J Adhes Sci Technol*, vol. 26, no. 4-5, pp. 447-461, 2012.

[3] H.-C. Dan, L.-H. He, J.-F. Zou, L.-H. Zhao, and S.-Y. Bai, "Laboratory study on the adhesive properties of ice to the asphalt pavement of highway," *Cold Reg. Sci. Technol.*, vol. 104-105, pp. 7-13, 2014.

[4] S. K. Thomas, R. P. Cassoni, and C. D. MacArthur, "Aircraft anti-icing and de-icing techniques and modeling," *J. Airc.*, vol. 33, no. 5, pp. 841-854, 1996.

[5] H. Habibi, L. Cheng, H. Zheng, V. Kappatos, C. Selcuk, and T.-H. Gan, "A dual de-icing system for wind turbine blades combining high-power ultrasonic guided waves and low-frequency forced vibrations," *Renew. Energy*, vol. 83, no. 2, pp. 859-870, 2015.

[6] M. J. Kreder, J. Alvarenga, P. Kim, and J. Aizenberg, "Design of anti-icing surfaces: smooth, textured or slippery?," *Nat. Rev. Mater.*, vol. 1, no. 1, p. 15003, 2016.

[7] S. Tarquini, C. Antonini, A. Amirfazli, M. Marengo, and J. Palacios, "Investigation of ice shedding properties of superhydrophobic coatings on helicopter blades," *Cold Reg. Sci. Technol.*, vol. 100, no. 6, pp. 50-58, 2014.

[8] W. Barthlott and C. Neinhuis, "Purity of the Sacred Lotus, or Escape from contamination in biological surfaces," *Planta*, vol. 202, no. 1, pp. 1-8, 1997.

[9] V. Vercillo *et al.*, "Design rules for laser-treated icephobic metallic surfaces for aeronautic applications," *Adv. Funct. Mater.*, vol. 30, no. 16, p. 1910268, 2020.

[10] K. K. Varanasi, T. Deng, J. D. Smith, M. Hsu, and N. Bhate, "Frost formation and ice adhesion on superhydrophobic surfaces," *Appl. Phys. Lett.*, vol. 97, no. 23, p. 234102, 2010.

[11] R. Dou *et al.*, "Anti-icing coating with an aqueous lubricating layer," *ACS Appl. Mater. Interfaces*, vol. 6, no. 10, pp. 6998-7003, 2014.

[12] L. Zhu, J. Xue, Y. Wang, Q. Chen, J. Ding, and Q. Wang, "Ice-phobic coatings based on silicon-oil-infused polydimethylsiloxane," *ACS Appl. Mater. Interfaces*, vol. 5, no. 10, pp. 4053-4062, 2013.

[13] T.-S. Wong *et al.*, "Bioinspired self-repairing slippery surfaces with pressure-stable omniphobicity," *Nature*, vol. 477, no. 7365, pp. 443-447, 2011.

[14] P. Kim, T.-S. Wong, J. Alvarenga, M. J. Kreder, W. E. Adorno-Martinez, and J. Aizenberg, "Liquid-infused nanostructured surfaces with extreme anti-ice and anti-frost performance," *ACS Nano*, vol. 6, no. 8, pp. 6569-6577, 2012.

[15] M. J. Coady *et al.*, "Icephobic behavior of UV-cured polymer networks incorporated into slippery lubricant-infused porous surfaces: improving SLIPS durability," *ACS Appl. Mater. Interfaces*, vol. 10, no. 3, pp. 2890-2896, 2018.

[16] K. Golovin, A. Dhyani, M. D. Thouless, and A. Tuteja, "Low–interfacial toughness materials for effective large-scale deicing," *Science*, vol. 364, no. 6438, p. 371, 2019.

[17] P. Irajizad *et al.*, "Stress-localized durable icephobic surfaces," *Mater. Horiz.*, vol. 6, no. 4, pp. 758-766, 2019.

[18] Z. He, S. Xiao, H. Gao, J. He, and Z. Zhang, "Multiscale crack initiator promoted super-low ice adhesion surfaces," *Soft Matter*, vol. 13, no. 37, pp. 6562-6568, 2017.

[19] Z. He, Y. Zhuo, F. Wang, J. He, and Z. Zhang, "Understanding the role of hollow sub-surface structures in reducing ice adhesion strength," *Soft Matter*, vol. 15, no. 13, pp. 2905-2910, 2019.

[20] Z. He, Y. Zhuo, F. Wang, J. He, and Z. Zhang, "Design and preparation of icephobic PDMS-based coatings by introducing an aqueous lubricating layer and macro-crack initiators at the ice-substrate interface," *Prog. Org. Coat.*, vol. 147, p. 105737, 2020.

[21] E. J. Y. Ling, V. Uong, J.-S. Renault-Crispo, A.-M. Kietzig, and P. Servio, "Reducing ice adhesion on nonsmooth metallic surfaces: wettability and topography effects," *ACS Appl. Mater. Interfaces*, vol. 8, no. 13, pp. 8789-8800, 2016.

[22] K. Alasvand Zarasvand, C. Pope, M. Mohseni, D. Orchard, C. Clark, and K. Golovin, "Metallic plate buckling as a low adhesion mechanism for durable and scalable icephobic surface design," *Adv. Mater. Interfaces*, vol. 9, no. 1, p. 2101402, 2022.

[23] S. Wang *et al.*, "Icephobicity of penguins *spheniscus humboldti* and an artificial replica of penguin feather with air-infused hierarchical rough structures," *J. Phys. Chem. C*, vol. 120, no. 29, pp. 15923-15929, 2016.

[24] C. Dawson, J. F. V. Vincent, G. Jeronimidis, G. Rice, and P. Forshaw, "Heat transfer through penguin feathers," *J. Theor. Biol.*, vol. 199, no. 3, pp. 291-295, 1999.

[25] D. J. McCafferty, C. Gilbert, A. M. Thierry, J. Currie, Y. Le Maho, and A. Ancel, "Emperor penguin body surfaces cool below air temperature," *Biol. Lett.*, vol. 9, no. 3, p. 20121192, 2013.

[26] E. Alizadeh-Birjandi *et al.*, "Delay of ice formation on penguin feathers," *Eur. Phys. J.: Spec. Top.*, vol. 229, no. 10, pp. 1881-1896, 2020.

[27] G. Moreno-Rueda, "Preen oil and bird fitness: a critical review of the evidence," *Biol. Rev.*, vol. 92, no. 4, pp. 2131-2143, 2017.

[28] E. Bormashenko, Y. Bormashenko, T. Stein, G. Whyman, and E. Bormashenko, "Why do pigeon feathers repel water? Hydrophobicity of pennae, Cassie–Baxter wetting hypothesis and Cassie–Wenzel capillarity-induced wetting transition," *J. Colloid Interface Sci.*, vol. 311, no. 1, pp. 212-216, 2007.

[29] M. J. Wood, P. Servio, and A.-M. Kietzig, "The tuning of LIPSS wettability during laser machining and through post-processing," *Nanomaterials*, vol. 11, no. 4, p. 973, 2021.